JOURNAL OF Materials CHEMISTRY

New routes to transition metal nitrides: preparation and characterization of new phases†

Roger Marchand,*[a] Franck Tessier[a,b] and Francis J. DiSalvo[b]

[a]*Laboratoire Verres et Céramiques, UMR CNRS 6512, Université de Rennes 1, 35042 Rennes Cedex, France. E-mail: rmarchan@univ-rennes1.fr*
[b]*Department of Chemistry, Baker Laboratory, Cornell University, Ithaca, NY 14853-1301, USA*

Received 13th April 1998, Accepted 8th July 1998

Transition metal nitrides form a class of materials with unique physical properties which give them varied applications, as high temperature ceramics, magnetic materials, superconductors or catalysts. They are commonly prepared by high temperature conventional processes, but alternative synthetic approaches have also been explored, more recently, which utilize moderate-temperature conditions. For example, high surface area γ-Mo_2N nitride powders (fcc phase) are prepared from commercial oxide MoO_3 through a topotactic transformation process. Of prime importance is the nature of the precursor, because it may yield new nitride phases unattainable by other synthetic routes. A novel promising method to nitride synthesis has been developed using sulfides as starting materials. The ammonolysis reaction has been applied first to the preparation of two binary molybdenum nitrides: Mo_5N_6 (filled 2H-MoS_2 structure) and δ-MoN (NiAs-type structure) from MoS_2, and then extended to other metals such as W, Cr or Ti, as well as molybdenum- and tantalum-based ternary systems. Fine reactive molybdenum sulfide precursor powders ($S_g \geqslant 200\ m^2\ g^{-1}$) have been synthesized in thiocyanate melt. On the other hand, alkali metal ternary oxides offer potential as nitridation precursors. For example, a binary nitride Nb_4N_5 (defect NaCl-type structure) results from ammonolysis of sodium or potassium niobates whereas $LiNb_3O_8$ is transformed into a mixed valent ternary nitride $LiNb_3N_4$ (filled 2H-MoS_2 structure). Another illustration of the Li^+ inductive effect is given in the direct synthesis of $LiMN_2$ from Li_2MO_4 (M = Mo, W). The nitrides Mo_5N_6, δ-MoN and Nb_4N_5 show superconducting behavior at $T < 12$ K.

Nitrogen, which is located in the Periodic Table of the Elements between carbon and oxygen, gives rise to two main families of binary nitrides. Whereas the first ones are close to oxides with a more or less significant ionic or covalent character, the second ones, essentially transition metal nitrides, are metallic in character and similar to carbides, with nitrogen occupying interstitial positions of the metal atom arrangement. The transition metal nitrides form a class of materials with unique physical properties which give them a wide variety of applications, for example as high temperature ceramics, magnetic materials, superconductors or catalysts.[1–3]

The first syntheses of transition metal nitrides were derived from metallurgical processes, and consisted of nitriding the metal or the oxide under severe conditions, in particular at high temperatures (≥1500 K). Much later, the development of catalytic applications requiring high specific surface area nitride powders needed to utilize moderate-temperature synthetic conditions was achieved. In addition, in the past decade, research on nitrides has become very intensive, focusing mainly on the study of new ternary compositions, and novel synthetic approaches have been explored. This paper aims at illustrating that the use of different reaction conditions or novel precursors may lead to new preparation routes of binary or ternary transition metal nitrides. It deals, in particular, with the description of an original method using sulfides as nitridation precursors. Ammonolysis reactions of both commercial and high surface area molybdenum sulfide MoS_2 were first studied, leading to a new nitride composition Mo_5N_6 and to the nitride δ-MoN. This promising process for the preparation of nitrides was then extended to other binary transition metal sulfides as well as to more complex sulfides, illustrated here by CuM_2S_4 (M = Ti, Co), MMo_2S_4 (M = Ti, V, Cr, Mn, Fe, $Ga_{0.67}$) and M_xTaS_2 (M = Cu, Zn, Al, In, Sn) compositions. Finally, it is shown that alkaline ternary oxides are particularly appropriate for nitridation as starting products. The ammonolysis of alkaline niobates is described, yielding a new ternary nitride $LiNb_3N_4$ and also a binary Nb_4N_5.

Molybdenum nitrides

Molybdenum nitrides are subjected to intensive studies because of the high T_c (*ca.* 30 K)[4] predicted for a hypothetical B_1-MoN superconductor mononitride (of cubic NaCl-type; hitherto, the only known mononitride is the hexagonal δ-MoN, with a T_c of 15 K), and also because of the potential of the fcc γ-Mo_2N phase in heterogeneous catalysis for reactions traditionally catalyzed by noble metals.[5] This latter phase results from reaction between molybdenum trioxide MoO_3 and ammonia, and it can be obtained with a high specific surface area (commonly $120\ m^2\ g^{-1}$),[6–8] starting from low surface area commercial oxide powder (*ca.* $2\ m^2\ g^{-1}$), through a temperature-programmed reaction (TPR) method of preparation. This method, developed by Boudart's group at Stanford University for the preparation of several transition metal nitrides (and also carbides), consists of placing the oxide precursor in flowing ammonia while slowly and uniformly raising the temperature (to 700 °C in this case).[9] The transformation is topotactic as the (100) crystallographic planes of γ-Mo_2N are produced parallel to the original parent MoO_3 (010) planes. The reaction product, of lower density, consists of highly porous nitride platelets, as it is pseudomorphous with the original MoO_3.[5,10]

The other above-mentioned nitride δ-MoN is difficult to prepare in a pure state by the reaction between MoO_3 and NH_3. Depending on the reaction conditions, δ-MoN is often accompanied either by γ-Mo_2N or by Mo metal. Bezinge

†Basis of the presentation given at Materials Chemistry Discussion No. 1, 24–26 September 1998, ICMCB, University of Bordeaux, France.

Table 1 Experimental preparation conditions of Mo_5N_6 and MoN. Nitrogen and oxygen analysis results

	Mo_5N_6	MoN
Amount of commercial MoS_2/g	1	0.5
Rate of temperature increase/°C min^{-1}	15	15
NH_3 flow rate/l h^{-1}	35	35
Final temperature/°C	750	850
Step time/h	96	20
Oxygen content (wt.%)	0.8	0.5_5
Nitrogen content: obs. (wt.%)	15.0	13.2
calc. (wt.%)	14.91	12.74

et al.[11] used severe temperature and pressure conditions (1800 K, 6 GPa) for its direct synthesis from the constituent elements.

Ammonolysis of MoS_2

In contrast, the ammonolysis of molybdenum sulfide MoS_2 yields pure δ-MoN at moderate temperature ($T \leqslant 850$ °C and ambient pressure). Moreover, such a novel method of synthesis allows a new molybdenum nitride, Mo_5N_6, unattainable by other synthetic routes, to be prepared. The reactions are:

$$MoS_2 + 4/3\ NH_3 \rightarrow 1/5\ Mo_5N_6 + 2\ H_2S^{\uparrow} + 1/15\ N_2^{\uparrow}$$

$$MoS_2 + 4/3\ NH_3 \rightarrow MoN + 2\ H_2S^{\uparrow} + 1/6\ N_2^{\uparrow}$$

in which sulfur is eliminated as H_2S gas. Table 1 gathers the experimental conditions used when starting from commercial molybdenite (2H-MoS_2, 3 $m^2\ g^{-1}$), as well as results of nitrogen and oxygen analysis provided simultaneously by a LECO analyzer, nitrogen being measured as N_2 in a thermal conductivity cell and oxygen as CO_2 by infrared detection. In all experiments the amount of oxygen is found to be very low ($\ll 1\%$). Both compounds are totally free from sulfur as shown by negative determinations as SO_2. The nitrogen-richer nitride Mo_5N_6 is prepared at a lower temperature (750 °C) than MoN (850 °C). The corresponding specific surface areas are increased with respect to the precursor, 16 and 7 $m^2\ g^{-1}$ for Mo_5N_6 and MoN, respectively. These values do not change significantly with the rate of temperature increase.[12]

High surface area MoS_2 precursor

Previous work by Milbauer[13] and, more recently, by Kerridge and Walker,[14,15] has shown that different oxides can react in molten alkaline thiocyanates to give sulfides. In particular, molybdenum sulfides were obtained at 300 °C in KSCN melt (mp = 177 °C) from MoO_3 or Na_2MoO_4. The equation of reaction written by Kerridge and Walker for MoO_3 is:

$$3\ MoO_3 + 5\ SCN^- \rightarrow Mo_2S_3 + MoS_2 + 5\ OCN^- + 2\ O_2^{\uparrow}$$

These first results were optimized in order to prepare a reactive MoS_2 precursor powder and an experimental procedure was defined based upon the transformation of MoO_3 which gives the best results. A fine MoS_2 powder with a specific surface area as high as 200 $m^2\ g^{-1}$ is prepared as follows: a homogeneous mixture of MoO_3 and KSCN with a large excess of KSCN is slowly heated (1 °C min^{-1}) to 350 °C in a muffle furnace. A black solid forms between 200 and 300 °C. After maintaining the temperature for 15 h and cooling, the sponge-like product is crushed and thoroughly washed with water then alcohol and finally dried for a few hours at 60 °C, then at 110 °C under vacuum. Pure MoS_2 is obtained under these conditions. Fig. 1 shows the poorly crystalline X-ray diagram of MoS_2 compared to that of commercial MoS_2. The morphology of the powder is shown by the SEM micrograph of Fig. 2.

Apart from the fact that such a high surface area MoS_2 powder has, itself, potential applications in heterogeneous catalysis (studies are in progress), it shows an interesting reactivity with ammonia. It is possible to prepare pure Mo_5N_6 nitride at $T < 700$ °C with a high specific surface area of 50 $m^2\ g^{-1}$. The relative decrease in surface area is only due to the ammonolysis reaction, the surface area of MoS_2 itself is not affected by thermal treatment under an ammonia atmosphere.[16]

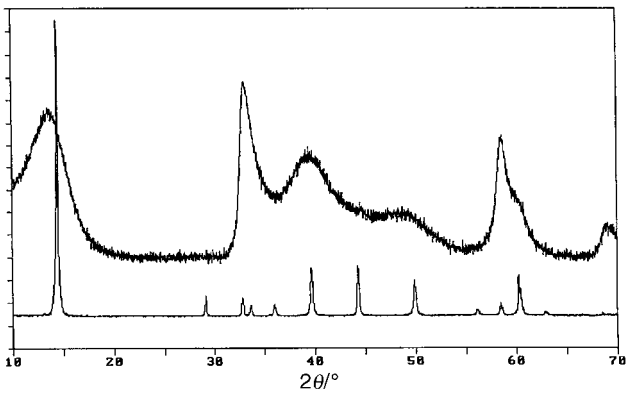

Fig. 1 X-Ray powder diffraction pattern (Cu-Kα) of a high surface area MoS_2 powder compared with commercial MoS_2. (Preferential orientations are observed due to the bidimensional character of the products.)

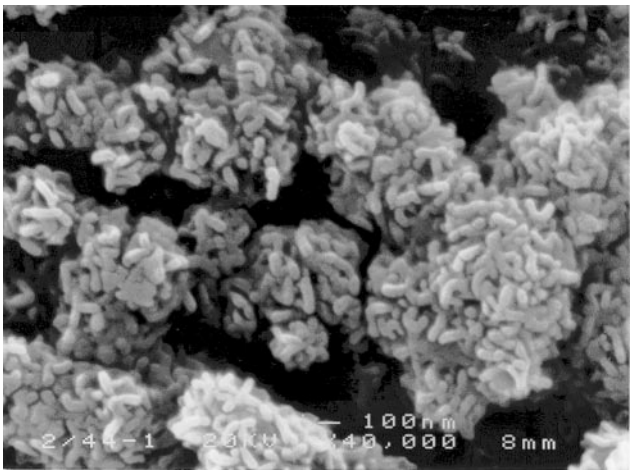

Fig. 2 SEM micrograph (×40 000) of a high surface area MoS_2 powder (specific surface area $S_g = 194\ m^2\ g^{-1}$, specific pore volume $V_g = 1.31\ cm^3\ g^{-1}$).

Characterization of the nitrides MoN and Mo_5N_6

The X-ray powder diffraction pattern of MoN is similar to that of δ-MoN reported in the JCPDS files, except for the presence of a few extra weak peaks which can be indexed in the δ-MoN hexagonal unit cell (Table 2). The neutron diffraction refined parameters, compared with previous values indicated between brackets, are: $a = 5.733(2)$ Å ($a = 5.745$ Å), $c = 5.613(2)$ Å ($c = 5.622$ Å), $Z = 8$. The crystal structure refinement from neutron diffraction data, which is necessary to determine the nitrogen positions, corroborates the results of Bezinge *et al.*[11] in the space group $P6_3mc$. The structure can be described as a distorted NiAs-type arrangement with some of the molybdenum atoms forming triangular metallic clusters, as shown in Fig. 3, in which the Mo–Mo distances are shorter (2.67 Å) than in Mo metal (2.80 Å).

The X-ray powder diffraction pattern of Mo_5N_6 has been indexed in a hexagonal unit cell with the parameters (Table 3): $a = 4.893(1)$ Å, $c = 11.06(1)$ Å, $Z = 2$, which can be compared to the unit cell parameters of MoN: $a_{Mo_5N_6} \approx a_{MoN} \times (\sqrt{3})2$, $c_{Mo_5N_6} \approx c_{MoN} \times 2$ ($V_{Mo_5N_6} \approx V_{MoN} \times 3/2$). The crystal structure

Table 2 X-Ray powder diffraction data for δ-MoN [λ(Cu-Kα) = 1.5418 Å]

h k l	$2\theta_{obs.}$/°	$2\theta_{calc.}$/°	$d_{obs.}$/Å	I/I_0
101	24.000	23.908	3.7049	2
002	31.880	31.858	2.8049	62
200	36.215	36.154	2.4784	100
201	39.665	39.666	2.2704	2
202	48.915	48.944	1.8605	74
211	51.300	51.292	1.7795	3
103	52.240	52.199	1.7497	<1
301	58.110	58.057	1.5861	2
203	62.035	62.063	1.4949	<1
220	65.010	65.019	1.4334	11
302	65.515	65.412	1.4236	4
004	66.567	66.582	1.4036	8
213	71.080	71.091	1.3252	<1
222	74.196	74.236	1.2771	10
400	76.635	76.718	1.2424	5
204	78.143	78.178	1.2221	13
402	85.398	85.463	1.1359	8
321	87.205	87.268	1.1169	1

$a = 5.733(2)$ Å, $c = 5.613(2)$ Å, $V = 159.8$ Å^3.

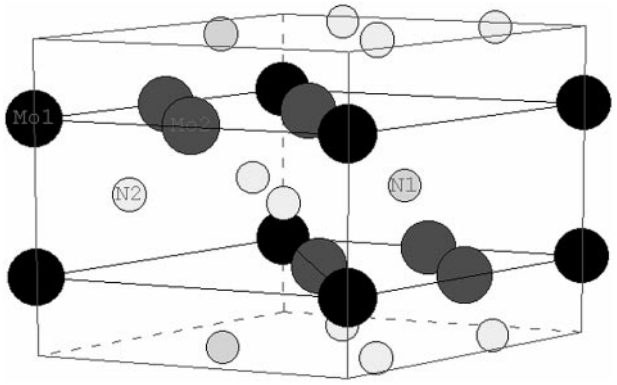

Fig. 3 δ-MoN hexagonal unit cell. Large circles represent Mo atoms. Triangular Mo clusters are shown.

Table 3 X-Ray powder diffraction data for Mo_5N_6 [λ(Cu-Kα) = 1.5418 Å]

h k l	$2\theta_{obs.}$/°	$2\theta_{calc.}$/°	$d_{obs.}$/Å	I/I_0
002	16.015	16.013	5.5297	7
100	21.030	20.947	4.2201	2
101	22.405	22.450	3.9649	4
004	32.320	32.350	2.7677	25
110	36.710	36.703	2.4461	100
111	37.665	37.623	2.3863	3
112	40.265	40.276	2.2380	4
201	43.505	43.452	2.0785	1
113	44.585	44.403	2.0307	1
114	49.710	49.719	1.8326	70
115	56.075	55.997	1.6388	<1
211	58.125	58.150	1.5857	1
116	63.005	63.094	1.4742	1
300	66.115	66.095	1.4121	17
008	67.665	67.717	1.3835	4
302	68.550	68.505	1.3678	1
304	75.515	75.521	1.2580	12
220	78.000	78.055	1.2240	7
118	79.600	79.576	1.2034	9
311	82.420	82.462	1.1692	<1
224	86.980	87.033	1.1192	11

$a = 4.893(1)$ Å, $c = 11.06(1)$ Å, $V = 229.3$ Å^3.

has been determined by neutron diffraction using the Rietveld method. The results show a close correspondence between this bulk material and a molybdenum–nitrogen phase $Mo_{0.82}N$–$Mo_{0.85}N$ prepared as a thin film by Troitskaya and Pinsker,[17] and characterized by electron diffraction with the

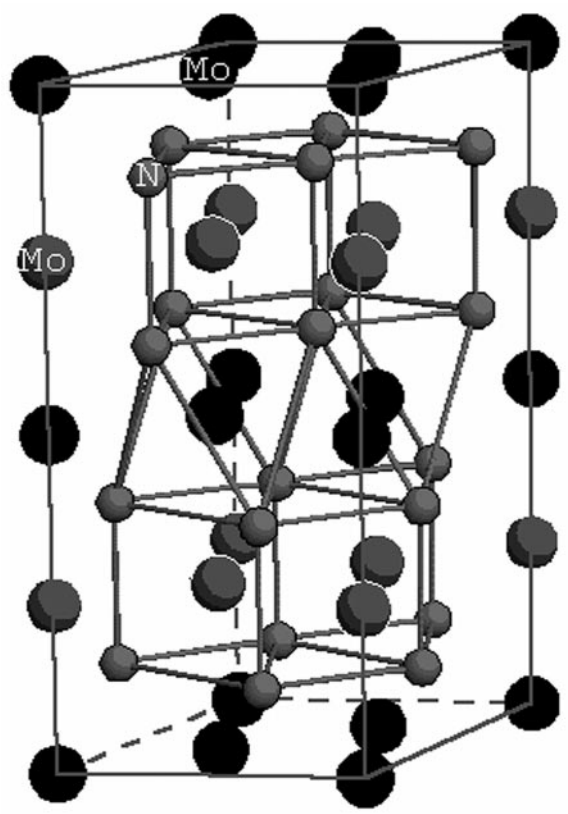

Fig. 4 Mo_5N_6 hexagonal unit cell showing alternate prisms and octahedra formed by nitrogen atoms along the *c* axis.

hexagonal parameters: $a = 2.86$ Å ($\approx a_{Mo_5N_6}/\sqrt{3}$), $c = 11.20$ Å ($\approx c_{Mo_5N_6}$).

The structure of Mo_5N_6 consists of alternate layers of nitrogen prisms and octahedra along the *c* axis, as shown in Fig. 4, the nitrogen atoms forming an AABB-type arrangement, like the sulfur atoms in MoS_2. The molybdenum atoms occupy all the trigonal prismatic sites while the octahedral sites are only partially (2/3) occupied. Therefore, the Mo_5N_6 structure can be considered as a filled 2H-MoS_2 structure and the unit cell content is $(Mo_4\square_2)_{(octa)}[Mo_{6(prism)}N_{12}]$. The distribution of Mo atoms and vacancies in the octahedral sites has not yet unambiguously been determined (space group $P6_3/m$ or $P6_322$).[12]

In addition, let us note the morphological analogy between the Mo_5N_6 nitride powder and its commercial MoS_2 precursor, as highlighted by the SEM micrograph of Fig. 5 where a characteristic lamellar structure can be seen.

For both nitrides, MoN and Mo_5N_6, magnetic susceptibility measurements in low magnetic field (SQUID, $H = 10^{-3}$ T, zero field cooled) have been carried out which show that both compounds exhibit superconducting behavior at $T < 12$ K (Fig. 6).

Finally, the two nitrides show different behavior towards aging. Whereas Mo_5N_6 powder is very stable in moist air, it has been observed surprisingly that MoN powder slowly transforms into $MoO_3 \cdot xNH_3 \cdot yH_2O$ phases.

Ammonolysis of other sulfide precursors

The thermal ammonolysis of sulfides as a novel method for the synthesis of nitride-type compounds has been developed and extended to other binary, but also more complex sulfides. In particular, the preparation of new ternary transition metal nitrides from corresponding ternary sulfide compositions has

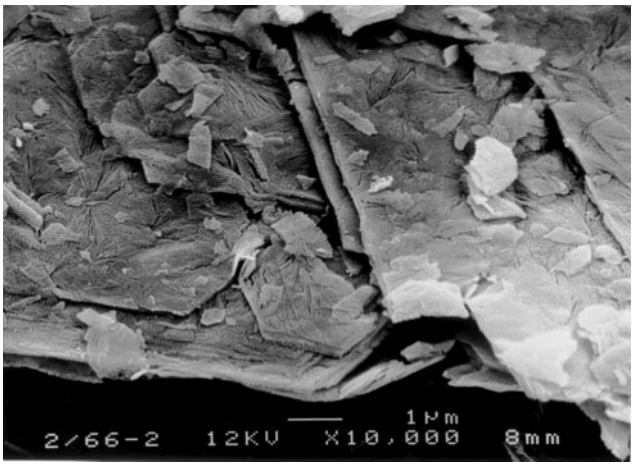

Fig. 5 SEM micrograph (×10 000) of a Mo_5N_6 powder resulting from ammonolysis of commercial MoS_2.

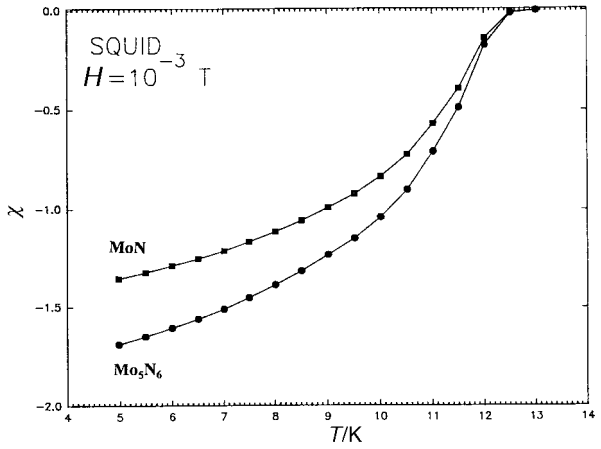

Fig. 6 $\chi = f(T)$ curves for MoN and Mo_5N_6.

been envisaged according to the general reaction scheme :

$$MM'S_x + 2x/3\ NH_3 \rightarrow MM'N_y + xH_2S^{\uparrow} + (x/3 - y/2)N_2^{\uparrow}$$

where M and/or M' represent(s) a transition metal.

All the nitridation reactions were carried out in an alumina boat placed inside a quartz tube through which commercial ammonia gas flowed at a rate of 30–40 l h^{-1}. Sodium pieces were used to dehydrate the nitriding gas. The temperature was raised to the range 700–850 °C, depending on the starting sulfide, generally with a heating rate of 5 °C min^{-1}. The samples were held at their respective temperature for 2 days. The furnace was then switched off and the powder was allowed to cool to room temperature under nitrogen atmosphere.

Binary sulfides

WS_2 reacts with NH_3, however utilization of a reactive tungsten sulfide powder is very important in this case since commercial WS_2 (2 m^2 g^{-1}) is not able to lead to a pure nitride phase, free from tungsten metal.[18] It is possible to prepare a more reactive precursor powder with an optimized high specific surface area of 30 m^2 g^{-1} when heating WO_3 at 550 °C in molten NaSCN (mp = 287 °C), according to a similar procedure to that described above. The tungsten nitride which forms in flowing ammonia between 750 and 850 °C is a new compound, of composition W_5N_6, which is not isostructural with Mo_5N_6 and whose hexagonal parameters are: a = 5.014(8) Å, c = 15.26(3) Å.

Early transition metal sulfides, Cr_2S_3 and TiS_2[18,19] as well as VS_2,[19] also react with ammonia, as low as 600 °C, to give rise to nitride phases. Depending on the purity, in particular of the NH_3 gas flow, cubic NaCl-type oxynitride phases or nitrides (CrN, TiN, VN) are obtained with a surface area and a crystallization state closely related to the nitridation temperature: the lower the temperature, the higher the surface area, correlated with a poor crystallization state.

Ternary sulfides

It is well known that nitrogen-rich transition metal nitrides are not stable at elevated temperatures, in particular because of the great stability of the dinitrogen molecule (high bond energy of 941 kJ mol^{-1}). Under these conditions, ternary sulfides are much more appropriate than the corresponding oxides for reaction with ammonia at moderate temperatures in order to form new ternary nitride compositions. The first results reported in this work concern the thermal ammonolysis of ternary sulfides with stoichiometries CuM'_2S_4 (M' = Ti, Co), MMo_2S_4 (M = Ti, V, Cr, Mn, Fe, $Ga_{0.67}$ [or $GaMo_3S_6$]) and M_xTaS_2 (M = Cu, Zn, Al, In, Sn).

The same procedure was used to prepare all the precursors. Metal and sulfur powders, or sometimes metal and binary sulfide powders, were first ground intimately in a mortar, from which a pellet was pressed, a little excess of sulfur being added for each composition. The pellets were slowly heated under vacuum in sealed quartz tubes at temperatures between 800 and 1100 °C.

CuM'_2S_4 (M' = Ti, Co). Different behavior is observed for these two spinel-type sulfides when heated in flowing anhydrous ammonia. Whereas $CuTi_2S_4$ reacts with NH_3 as low as 600 °C to give rise at 700 °C to a well crystalline Cu + TiN mixture, the ammonolysis of $CuCo_2S_4$ leads at 700 °C to the formation of a new cubic nitrogen-containing ternary phase (Fig. 7); the composition is $CuCo_2N_{0.6}$ as determined by LECO nitrogen analysis (N wt.% experimental = 4.2). The value of the unit cell parameter a = 3.745(1) Å is noticeably higher than those of both metallic copper and cobalt. The parameters are compared in Table 4, as well as the positions of five characteristic F-type reflections of the XRD powder

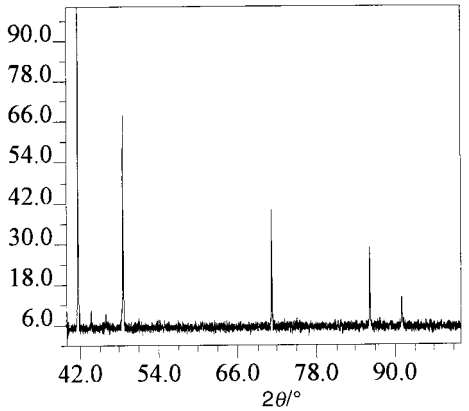

Fig. 7 X-Ray powder diffraction pattern (Cu-Kα) of $CuCo_2N_{0.6}$.

Table 4 Comparison between the XRD powder data and lattice parameters of $CuCo_2N_{0.6}$, Cu and Co.

	$CuCo_2N_{0.6}$		Cu		Co	
h k l	*d*/Å	I/I_0	*d*/Å	I/I_0	*d*/Å	I/I_0
111	2.1632	100	2.0880	100	2.0467	100
200	1.8729	68	1.8080	46	1.7723	40
220	1.3234	40	1.2780	20	1.2532	25
311	1.1284	29	1.0900	17	1.0688	30
222	1.0801	14	1.0436	5	1.0233	12
a/Å	3.745(1)		3.6150		3.5447	

patterns. When heated at 700 °C under argon atmosphere, $CuCo_2N_{0.6}$ decomposes into a Cu + Co mixture. At room temperature, the powder is magnetic, the observed saturation moment M_S is equal to 42 emu g^{-1}. Fig. 8 displays the corresponding hysteresis loops.

MMo_2S_4 (M = Ti, V, Cr, Mn, Fe, $Ga_{0.67}$). The results are gathered in Table 5. In no case is a ternary nitride composition detected; in general, mixtures of binary nitrides are found, except for gallium for which a new phase forms with a narrow thermal stability domain.

M_xTaS_2 (M = Cu, Zn, Al, In, Sn). M_xTaS_2 phases were synthesized as previously described[20] by reacting TaS_2 and the M metal powder. TaS_2 was prepared in a bent quartz tube where tantalum wires, sulfur and a small amount of iodine were put together. The bent part of the vacuum-sealed tube was placed in the colder part of a tubular furnace so that the sulfur vapor pressure remained below a few atmospheres. The reaction sequence was chosen to prevent explosion: a slow increase to 900 °C, *i.e.* 24 h to reach 600 °C (24 h reaction step), then 24 h to reach 900 °C (36 h reaction step) and finally 10 h to return to room temperature. In order to homogenize the resulting product, the powder was ground and reheated at 900 °C.

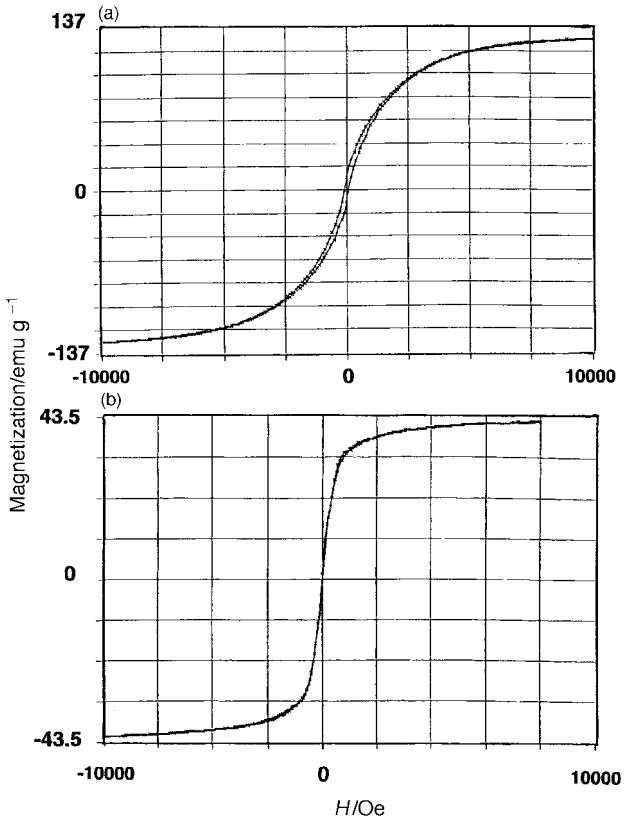

Fig. 8 Magnetic hysteresis loops of Co (a) and $CuCo_2N_{0.6}$ (b) powders.

Table 5 Ammonolysis of ternary molybdenum sulfides MMo_2S_4

Sulfide precursor	Temperature/ °C	XRD analysis
$TiMo_2S_4$ (+ε-$Mo_2S_3MoS_2$)	700	TiN + MoN
VMo_2S_4	700	VN + MoN
$CrMo_2S_4$	700	CrN + Mo_5N_6 (MoN)
$MnMo_2S_4$	750	MnS + Mo_5N_6
$FeMo_2S_4$ (+ε-MoS_2)	700	Mo_5N_6 (MoN) + ?
$Ga_{0.67}Mo_2S_4$	800	Precursor + new phase
	850	γ-Mo_2N + $GaMo_3$ + GaN

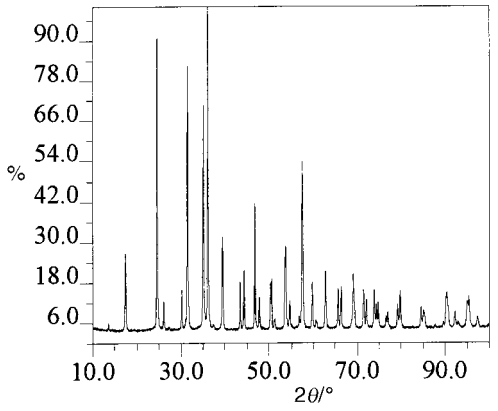

Fig. 9 X-Ray powder diffraction pattern (Cu-Kα) of the new Cu/Ta/N phase.

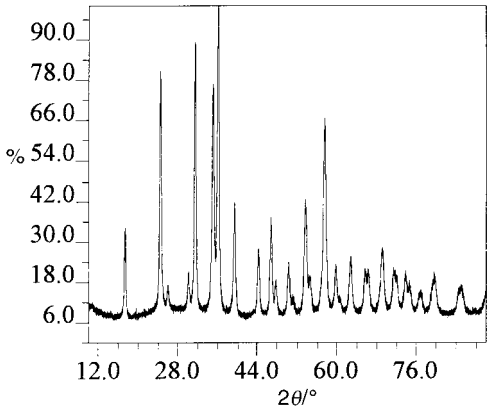

Fig. 10 X-Ray powder diffraction pattern (Cu-Kα) of the new Zn/Ta/N phase.

The binary tantalum sulfide TaS_2 is decomposed by ammonia at 700 °C to give the ionic covalent Ta^V nitride Ta_3N_5 of characteristic orange–red color, according to the reaction:

$$3\ TaS_2 + 5\ NH_3 \rightarrow Ta_3N_5 + 6\ H_2S^{\uparrow} + 3/2\ H_2^{\uparrow}$$

The nitriding character of NH_3 is preponderant in this case over its reducing character.

$Cu_{0.67}TaS_2$ reacts in flowing ammonia at 750 °C to yield an orange powder of composition $Cu_2Ta_3N_y$; a negative test with nitric acid concludes that no free Cu metal is present with the nitride powder. The orthorhombic unit cell: $a = 3.626(1)$ Å, $b = 5.101(1)$ Å, $c = 10.265(1)$ Å, is closely related to that of Ta_3N_5 (Fe_2TiO_5 pseudobrookite-type structure)[21]: $a' = 3.886$ Å, $b' = 10.212$ Å $\approx 2b$, $c' = 10.262$ Å $\approx c$ (Fig. 9).

When $Zn_{0.5}TaS_2$ is heated at 700 °C under flowing ammonia, there is partial evaporation of zinc and formation of a dark orange orthorhombic phase $Zn_xTa_3N_y$. As above, the orthorhombic unit cell can be compared with Ta_3N_5: $a = 3.643(3)$ Å, $b = 2.961(4)$ Å, $c = 10.260(8)$ Å (Fig. 10).

Experiments are also in progress with other M_xTaS_2 intercalation compounds, in particular with M = Al, In, Sn.

Niobium nitrides

One of the most common routes giving access to nitride-type compounds consists of the thermal ammonolysis of oxides. Pure nitrides and also oxynitrides can be synthesized by this method. The purpose here is to demonstrate that ternary oxides associating a transition metal with an alkali metal offer

interesting potential as nitridation precursors, because they can allow the synthesis of two kinds of new compounds, either binary transition metal nitrides or nitrogen-rich ternary nitrides. The first result is obtained after a total evaporation of the alkali metal, which will occur more easily when starting from sodium or potassium than from lithium compounds. In the second case, the Li^+ inductive effect is concerned. This concept, which is general in solid-state chemistry,[22–24] is based here on the donation of electron density from lithium to adjacent transition metal–nitrogen bonds, thereby increasing their covalent character and stability. Both cases are illustrated by alkaline niobates.[25]

Ternary nitride $LiNb_3N_4$

In contrast to $LiNbO_3$ which loses lithium when heated in flowing ammonia, leading to a NaCl-type Li–Nb–O–N oxynitride phase with variable lithium and nitrogen content,[26] no loss of lithium is detected for the niobate $LiNb_3O_8$ when ammonolyzed at a temperature as high as 1000 °C. This ternary oxide is easily transformed into a new ternary nitride $LiNb_3N_4$ with elimination of oxygen as water vapor, according to:

$$LiNb_3O_8 + 16/3\ NH_3 \rightarrow LiNb_3N_4 + 8\ H_2O^{\uparrow} + 2/3\ N_2^{\uparrow}$$

Table 6 gathers the corresponding XRD powder data. $LiNb_3N_4$, which is isotypic with a tantalum phase $Li_{1-x}Ta_{3+x}N_4$,[27] crystallizes hexagonally: $a = 5.2023(5)$ Å, $c = 10.363(1)$ Å, $Z = 3$.

Let us note that $Li_{1-x}Ta_{3+x}N_4$ was prepared from hygroscopic Li_3N (or $LiNH_2$)/Ta_3N_5 mixtures.

The crystal structure of $LiNb_3N_4$ (space group $P6_3/mcm$) consists of an AABB arrangement of nitrogen atoms, the stacking sequence along [001] is AαAγBβBγ where α and β represent trigonal prismatic sites and γ octahedral sites. On the basis of an ionic model: $Li^+Nb^{5+}Nb_2^{3+}N_4$, trivalent niobium Nb^{3+} is assigned to trigonal prismatic coordination, forming with nitrogen $(NbN_2)^{3-}$ layers, while Li^+ and pentavalent niobium Nb^{5+} are intercalated between the layers in octahedral holes (Fig. 11). In this way $LiNb_3N_4$ is very close to the previously described molybdenum nitride Mo_5N_6, the formula is written for better comparison as $\square_{0.67}Mo_3N_4$. The mixed valent ternary nitride $LiNb_3N_4$ shows characteristic semiconducting behavior.[12]

In this connection, let us add the syntheses of the two isostructural compounds $LiMoN_2$ [28] and $LiWN_2$ [29] by ammonolysis of Li_2MoO_4 and Li_2WO_4. They constitute another example of transformation of a ternary oxide into a ternary nitride in which the electropositive element Li has a stabilizing effect.

Binary nitride Nb_4N_5

A convenient method of synthesizing the binary niobium nitride Nb_4N_5 as a bulk material consists of ammonolyzing at 800 °C sodium or potassium niobate $NaNbO_3$ or $KNbO_3$. Sodium or potassium totally evaporates under these conditions and Nb_4N_5 forms according to:

$$4\ Na(K)NbO_3 + 8\ NH_3 \rightarrow Nb_4N_5 + \text{`}Na_3(K_3)N\text{'}^{\uparrow} + 12\ H_2O^{\uparrow} + 5/6\ N_2^{\uparrow}$$

This nitride had been previously identified as thin films after placing metal[30] or cubic nitride[31] thin films in a nitriding atmosphere. Ammonolysis of $NbCl_5$ is also possible.[32–33]

The XRD powder pattern of Nb_4N_5 can be indexed in a tetragonal unit cell (Table 7) with the parameters: $a = 6.853(1)$ Å, $c = 4.270(2)$ Å, $Z = 2$.

Nb_4N_5 is isotypic with Ta_4N_5[34,35] and Ti_4O_5.[36] The crystal structure has been refined in the space group $I4/m$ using the Rietveld method (Table 8). It is a defect NaCl-type structure with niobium vacancies, which is closely related to that of the B_1-type mononitride δ-NbN. The correspondence between the tetragonal Nb_4N_5 and the cubic δ-NbN unit cells is illustrated in Fig. 12. Calculated values of the small unit cell dimensions are: $a_o = a_{Nb_4N_5}[(\sqrt{10})2] = 4.334$ Å, $c_o = c_{Nb_4N_5} = 4.270$ Å (δ-NbN: $a = 4.392$ Å). They indicate a slight compression of the lattice along the c axis.

Table 6 X-Ray powder diffraction data for $LiNb_3N_4$ [λ(Cu-Kα) = 1.5418 Å]

$h\ k\ l$	$2\theta_{obs.}$/°	$2\theta_{calc.}$/°	$d_{obs.}$/Å	I/I_0
002	17.140	17.099	5.1692	20
100	19.695	19.689	4.5040	5
102	26.135	26.191	3.4069	5
004	34.615	34.595	2.5892	37
111	35.575	35.555	2.5215	60
112	38.730	38.703	2.3231	100
200	40.035	39.992	2.2503	2
113	43.540	43.519	2.0769	70
114	49.630	49.625	1.8354	1
006	53.005	52.975	1.7262	1
204	53.910	53.891	1.6993	1
115	56.760	56.745	1.6206	22
300	61.725	61.718	1.5016	31
116	64.725	64.737	1.4391	17
214	65.590	65.548	1.4222	1
206	68.320	68.389	1.3718	<1
304	72.700	72.723	1.2996	18
008	72.990	72.978	1.2952	14
221	73.275	73.300	1.2908	8
117	73.540	73.554	1.2868	8
222	75.265	75.273	1.2616	9
223	78.535	78.254	1.2170	8
306	85.665	85.643	1.1330	1
225	88.740	88.731	1.1015	5
119	94.020	94.044	1.0531	2
226	95.715	95.706	1.0389	4
316	99.060	99.084	1.0126	<1
308	103.515	103.500	0.9808	10

$a = 5.2023(5)$ Å, $c = 10.363(1)$ Å, $V = 242.9$ Å^3.

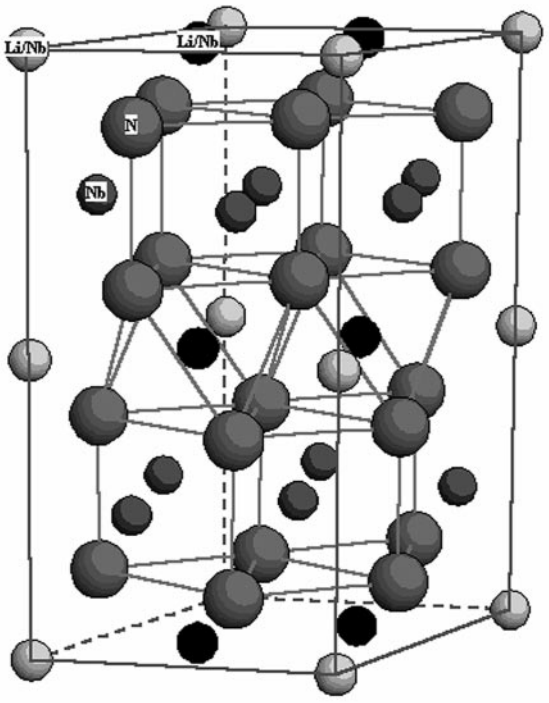

Fig. 11 $LiNb_3N_4$ hexagonal unit cell showing alternate nitrogen prisms and octahedra (large spheres).The prismatic Nb atoms are the white spheres, the octahedral (Li + Nb) atoms the black and dark gray spheres.

Table 7 X-Ray powder diffraction data for Nb_4N_5 [λ(Cu-Kα) = 1.5418 Å]

h k l	$2\theta_{obs.}$/°	$2\theta_{calc.}$/°	$d_{obs.}$/Å	I/I_0
110	18.414	18.293	4.8143	6
101	24.644	24.543	3.6096	23
200	26.094	25.983	3.4122	11
211	36.127	36.043	2.4843	100
220	37.161	37.075	2.4175	3
310	41.743	41.642	2.1621	66
002	42.336	42.296	2.1332	28
301	45.054	44.968	2.0106	1
112	46.491	46.438	1.9517	2
202	50.354	50.313	1.8107	4
321	52.729	52.669	1.7346	7
330	57.016	56.964	1.6139	1
222	57.513	57.485	1.6012	2
411	59.682	59.646	1.5480	5
420	60.428	60.355	1.5307	16
312	60.869	60.857	1.5207	31
103	67.082	67.108	1.3941	1
510	69.967	69.940	1.3435	2
431/501	72.361	72.350	1.3049	17
213	73.212	73.267	1.2918	8
422	76.408	76.450	1.2455	11
521	78.311	78.339	1.2199	3
440	78.943	78.966	1.2117	1
530	81.894	81.902	1.1754	1
323	85.027	85.080	1.1399	2
620	90.523	90.616	1.0844	4

$a = 6.853(1)$ Å, $c = 4.270(2)$ Å, $V = 200.5$ Å^3.

Table 8 Nb_4N_5 structure: atomic coordinates and refinement results

Atom	Site	*x*	*y*	*z*	B_{iso}/Å^2
Nb	8 (h)	0.2138(6)	0.3949(6)	0	0.38(12)
N(1)	8 (h)	0.303(5)	0.095(6)	0	0.4(4)
N(2)	2 (b)	0	0	0.5	0.4(4)

$R_p = 0.114$, $R_{wp} = 0.150$, $\chi^2 = 5.43$ for 85 recorded reflections.

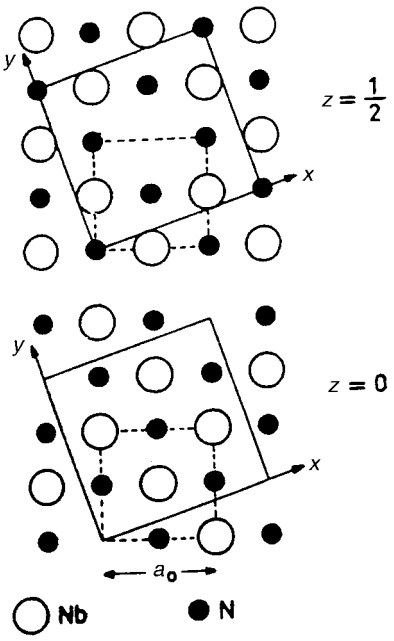

Fig. 12 Views of the Nb_4N_5 structure along [001] at $z = 0$ and $z = 1/2$.

The temperature-dependent magnetic susceptibility of Nb_4N_5 reveals a superconducting transition at $T_c \approx 10$ K. The curve of the electrical resistivity in zero magnetic field, plotted in Fig. 13, shows the sharp transition and the metallic character of the compound.

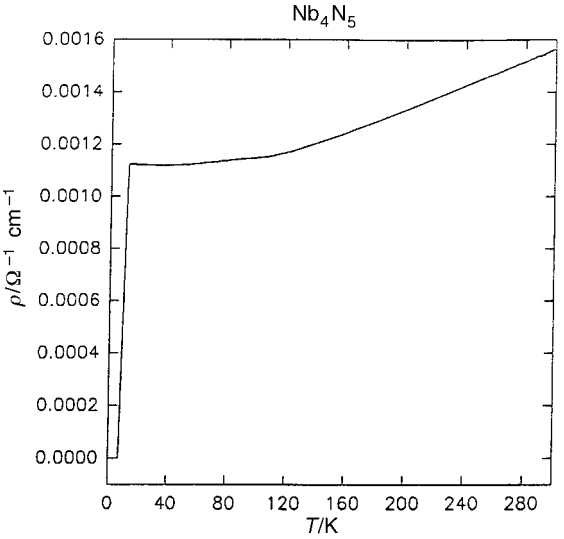

Fig. 13 Electrical resistivity, as a function of temperature, of a compacted bar of Nb_4N_5 powder, after annealing at 850 °C under a pure NH_3 atmosphere.

Conclusions

Great advances have been made in the last decade in research on new nitride compositions; the synthesis is more difficult than the synthesis of oxides. In particular, novel synthetic routes to transition metal nitrides are of interest due to their technological importance. In this paper, we have described original and characteristic reactions showing how important is the nature of the nitridation precursor in the nitride formation. A novel method of nitride synthesis involving sulfide precursors has been explored. Ammonolysis of MoS_2 exemplifies that reaction products may be largely influenced by the type, the crystal structure and the morphology of the precursor: δ-MoN is easily prepared from MoS_2 whereas it is difficult to prepare from MoO_3; Mo_5N_6 is a new nitride unattainable from MoO_3, whose crystal structure and powder morphology are closely related to the starting sulfide. From this viewpoint, the precursor acts as a template for nitride formation. The important role of the precursor, and also of the reaction conditions, is clearly demonstrated when high surface area pseudomorphous platelets of Mo_2N are produced from MoO_3 through a topotactic transformation. The sulfide route has been extended to more complex sulfides. The first results of the ammonolysis of ternary sulfides appear to be quite promising despite some difficulties in stabilizing (in some cases) ternary nitride compositions. Lithium can have a stabilizing effect as illustrated by the direct transformation of $LiNb_3O_8$ into $LiNb_3N_4$. As for the other alkali metals, sodium and potassium, their volatile character under the nitridation conditions has been taken advantage of in order to prepare as a bulk material the binary nitride Nb_4N_5 from the ternaries $NaNbO_3$ and $KNbO_3$.

These examples illustrate the importance of the choice of precursors and preparation methods and encourage us to pursue an exploration of original syntheses aiming at characterizing new nitride materials.

The authors would like to thank Prof. C. Michel and Dr A. Maignan (ISMRA Caen, France) for carrying out the measurements of electrical resistivities and the determination of critical temperatures, Prof. Suzuki (Cornell University) for the generous use of magnetic equipment, as well as Dr E. Suard (ILL Grenoble, France) and Prof. P. Gravereau (ICMCB Pessac, France) for their contributions, respectively, in neutron diffraction and Rietveld analysis. The research work at Cornell

University was supported by the National Science Foundation under Grant DMR-9508522.

References

1 L. E. Toth, *Transition Metal Carbides and Nitrides, Refractory Materials*, ed. J. L. Margrave, Academic Press, New York and London, 1971, vol. 7.
2 P. Ettmayer and W. Lengauer, in *Encyclopedia of Inorganic Chemistry*, ed. R. B. King, John Wiley & Sons, Chichester, 1994, p. 2498.
3 S. T. Oyama, in *The chemistry of Transition Metal Carbides and Nitrides*, ed. S. T. Oyama, Blackie A & P, Glasgow, 1996, p. 1.
4 D. A. Papaconstantopoulos and W. E. Pickett, *Phys. Rev. B*, 1985, **31**, 7093.
5 S. T. Oyama, *Catal. Today*, 1992, **15**, 179.
6 X. Gouin, R. Marchand, P. L'Haridon and Y. Laurent, *J. Solid State Chem*., 1994, **109**, 175.
7 R. Marchand, X. Gouin, F. Tessier and Y. Laurent, *Mater. Res. Soc. Symp. Proc.* 1995, **368**, 15.
8 R. Marchand, X. Gouin, F. Tessier and Y. Laurent, in *The Chemistry of Transition Metal Carbides and Nitrides*, ed. S. T. Oyama, Blackie A & P, Glasgow, 1996, p. 252.
9 L. Volpe and M. Boudart, *J. Solid State Chem.,* 1985, **59**, 332.
10 L. Volpe and M. Boudart, *Catal. Rev. Sci. Eng*., 1985, **27**, 515.
11 A. Bezinge, K. Yvon, J. Müller, W. Lengauer and P. Ettmayer, *Solid State Commun.*, 1987, **63**, 141.
12 F. Tessier, Thesis, Rennes, 1996.
13 J. Milbauer, *Z. Anorg. Allg. Chem.*, 1904, **42**, 433.
14 D. H. Kerridge and S. J. Walker, *J. Inorg. Nucl. Chem.*, 1977, **39**, 1579.
15 D. H. Kerridge, in *The Chemistry of Nonaqueous Solvents*, ed. J. J. Lagowsky, Academic Press, New York, 1978, p. 269.
16 F. Tessier, R. Marchand and Y. Laurent, *J. Eur. Ceram. Soc*., 1997, **17**, 1825.
17 N. V. Troitskaya and Z. G. Pinsker, *Sov. Phys. Crystallogr*., 1964, **8**, 441.
18 F. Tessier and R. Marchand, *J. Alloys Compd*., 1997, **262–263**, 410.
19 P. Subramanya Herle, M. S. Hegde, N. Y. Vasanthacharya, S. Philip, M. V. Rama Rao and T. Sripathi, *J. Solid State Chem*., 1997, **134**, 120.
20 F. J. DiSalvo, G. W. Hull Jr., L. H. Schwartz, J. M. Voorhoeve and J. V. Waszczak, *J. Chem. Phys.*, 1973, **59**, 1922.
21 (*a*) N. E. Brese, M. O'Keeffe, P. Rauch and F. J. DiSalvo, *Acta Crystallogr*., *Sect C*, 1991, **47**, 2291; (*b*) N. E. Brese and M. O'Keeffe, in *Structures and Bonding*, Springer-Verlag, Berlin, 1992, p. 307.
22 J. Etourneau, J. Portier and F. Ménil, *J. Alloys Compd.*, 1992, **188**, 1.
23 F. J. DiSalvo, *Science*, 1990, **247**, 649.
24 H.-C. zur Loye, J. D. Houmes and D. S. Bem, in *The Chemistry of Transition Metal Carbides and Nitrides*, ed. S. T. Oyama, Blackie A & P., Glasgow, 1996, p. 154.
25 F. Tessier, R. Assabaa and R. Marchand, *J. Alloys Compd*., 1997, **262–263**, 512.
26 R. Assabaa-Boultif, R. Marchand and Y. Laurent, (*a*) *Ann. Chim. Fr.*, 1994, **19**, 39; (*b*) *Eur. J. Solid State Inorg. Chem.*, 1995, **32**, 1101.
27 Th. Brokamp and H. Jacobs, *J. Alloys Compd.*, 1992, **183**, 325.
28 S. H. Elder, L. H. Doerrer, F. J. DiSalvo, J. B. Parise, D. Guyomard and J. M. Tarascon, *Chem. Mater.*, 1992, **4**, 928.
29 P. Subramanya Herle, M. S. Hegde, N. Y. Vasanthacharya, J. Gopalakrishnan and G. N. Subbanna, *J. Solid State Chem.*, 1994, **112**, 208.
30 N. Terao, *J. Less-Common Met*., 1971, **23**, 159.
31 G. Oya and Y. Onodera, *Jpn. J. Appl. Phys.*, 1971, **10**, 1485.
32 A. Yajima, T. Arai, R. Matsuzaki and Y. Saeki, *Bull. Chem. Soc. Jpn*., 1984, **57**, 1582.
33 G. Oya and Y. Onodera, *J. Appl. Phys.*, 1974, **45**, 1389.
34 A. Fontbonne and J.C. Gilles, *Rev. Int. Hautes Tempér. Réfract.*, 1969, **6**, 181.
35 N. Terao, *Jpn. J. Appl. Phys.*, 1971, **10**, 248.
36 D. Watanabe, O. Terasaki, A. Jostsons and J.R. Castles, *J. Phys. Soc. Jpn.,* 1968, **25**, 292.

Paper 8/05315D